GEOPHYSICAL RESEARCH LETTERS, VOL. 28, NO. 14, PAGES 2791-2794, JULY 15, 2001

Radiative cooling by stratospheric water vapor: big differences in GCM results

V. Oinas[1], A. A. Lacis, D. Rind, D. T. Shindell, and J. E. Hansen
NASA Goddard Institute for Space Studies, 2880 Broadway, New York, NY 10025

Abstract. The stratosphere has been cooling by about 2K/decade at 30-60 km over the past several decades and by lesser amounts toward the tropopause. Climate model calculations suggest that stratospheric water vapor is an important contributor to the observed stratospheric cooling, but there are large differences among recent GCM simulations for prescribed changes in stratospheric water vapor, which point to problems with the current GCM treatment of the absorption and emission by stratospheric water vapor. We show that the correlated k-distribution treatment with sufficient resolution is capable of simulating accurately cooling by stratospheric water vapor. We obtain equilibrium cooling of about 0.3K that extends from 20 km to the top of the atmosphere, and adjusted radiative forcing of 0.12 Wm^{-2}, for a stratospheric water vapor increase of 0.7 ppmv which has been estimated for the period 1979-1997.

Introduction

Observations of the middle and upper stratosphere from satellites, sondes and lidars all show that temperatures at altitudes from 30-60 km have been cooling over the past two to three decades at the rate of about 2 K/decade [*Golitsyn et al., 1996; Dunkerton et al., 1998; Keckhut et al., 1999*]. Microwave Sounding Unit (MSU) channel 4 measurements [*Spencer and Christy, 1993*] sample a broad region of the stratosphere centered at the 80 mb pressure level and show cooling at this level to be 0.4 K/decade. Attempts to reconcile global climate data and model results [*Hansen et al., 1997a, 1998*], find the model *vs.* data discrepancy at the 80 mb pressure level to be insufficient model cooling by about 0.1 K per decade.

Stratospheric water vapor trends (for the ~5 year period 1992 to 1997) come from HALOE measurements [*Evans et al., 1998; Nedoluha et al., 1998*] and from ground based millimeter-wave measurements (WVMS) taken at Table Mountain, CA and at Lauder, New Zealand [*Nedoluha et al., 1998*]. Balloonsonde observations by Oltmans *et al.* [*2000*], which sample the lower stratospheric water vapor below 30 km, are available at Boulder, CO since 1980. Evans *et al.* give the global average H_2O trend as varying between 40 ppbv/yr near 30 km, to 90 ppbv/yr at 45-50 km, and 65 ppbv/yr at 65-70 km. Nedoluha *et al.* [*1998*] find the water vapor increase to be 129 ppbv/yr at 40-60 km altitude based on HALOE measurements, and 148 ppbv/yr based on the WVMS instruments. Meanwhile, Oltmans *et al.* [*2000*] obtain water vapor increases in the lower stratosphere ranging from 48 ppbv/yr at 18-20 km to 44 ppbv/yr at 24-26 km.

[1]Also at Rutgers University.

Paper number 2001GL013137.
0094-8276/01/2001GL013137$05.00

Forster and Shine [*1999*] infer a global mean rate of 40 ppbv/yr increase in stratospheric water vapor from the observed trend data for the time period 1979-1997, the same time period for which ozone change data are also available. For modeling purposes, they express the water vapor increase as being uniform above the tropopause, in the form of a 0.7 ppmv increase above a background level of 6.0 ppmv. The results of their GCM study show equilibrium cooling by about 0.8 K between 5 to 50 mb with a vertical distribution that is remarkably similar to the cooling attributable to stratospheric ozone depletion for the same time period. However, if the equilibrium cooling due to stratospheric water vapor were as large as 0.8 K, it would be too large to achieve closure between climate data and model results.

Radiation model differences

The real problem is the large disparity in stratospheric equilibrium response to prescribed changes in stratospheric water vapor between different GCM calculations. The nature of these differences is illustrated in Fig. 1 by the equilibrium cooling response taken from recent modeling results. Model sensitivity to stratospheric water vapor is compared for a uniform perturbation of a 0.7 ppmv water vapor increment added to a 6.0 ppmv background level, as in the Forster and Shine study. Forster and

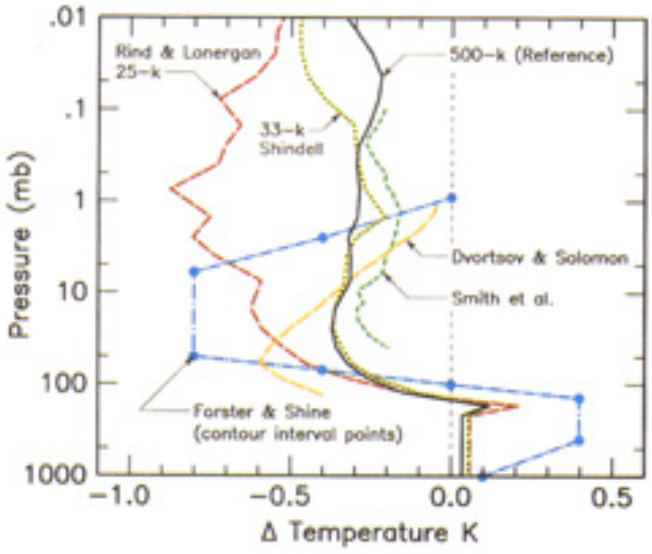

Figure 1. Equilibrium temperature change for a stratospheric water vapor increase from 6.0 to 6.7 ppmv above 150 mb. GCM sensitivity to stratospheric water vapor from Forster and Shine [1999] (blue dash-dot line). 1D RCM results using the radiation models used by Rind and Lonergan [1995] (red dashed line, 25-k) and Shindell [2001] (yellow dotted line, 33-k) are shown in comparison to the reference correlated k-distribution (solid black line, 500-k) results. Smith *et al.* [*2001*] model sensitivity is shown by the green dashed curve. Dvortsov and Solomon [*2001*] 2D model sensitivity is shown by the orange long-dash curve.

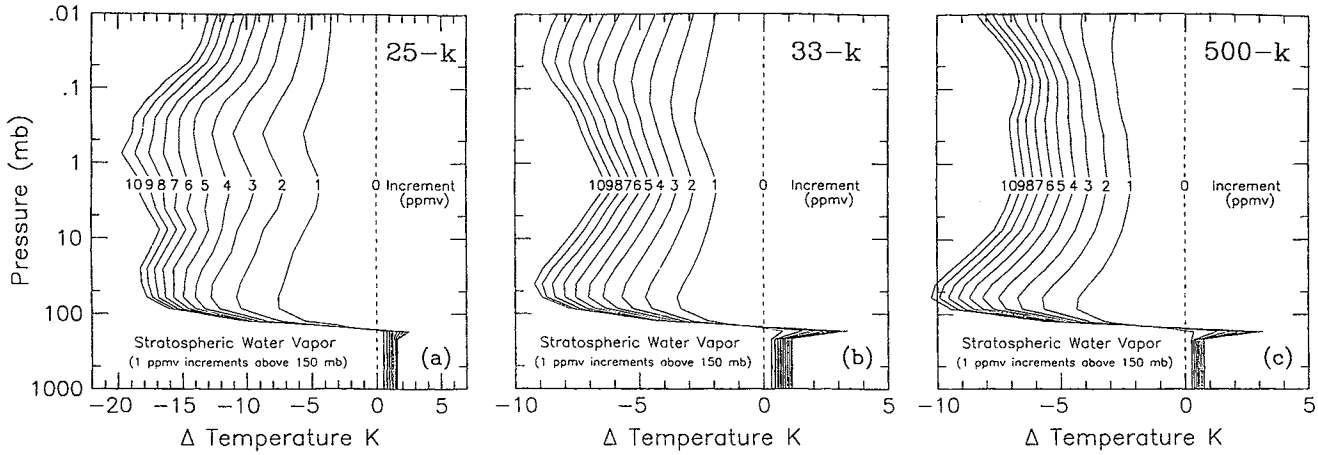

Figure 2. 1D RCM equilibrium temperature change for 1 ppmv additive increases of stratospheric water vapor applied uniformly above 150 mb. (a) 25 k-interval Model II version of GCM radiation model used by Rind and Lonergan [1995]. (b) 33 k-interval GCM radiation model used by Shindell [2001]. (c) 500-k numerical k-distribution benchmark. The reference water vapor is 0 for all curves. Note the change in scale for 25-k interval results.

Shine [*1999*] obtained equilibrium cooling of about 0.8 K between 5 and 50 mb (blue broken line) with the cooling falling sharply to zero above 1 mb and below the 100 mb level. These results are taken from the contour intervals of their Figure 1. The Smith *et al.* [*2001*] equilibrium cooling, shown by the green dashed curve, is taken from their Figure 3 and scaled linearly to a uniform 0.7 ppmv perturbation to yield a cooling of 0.2 to 0.3 K between 0.1 and 50 mb. (The cooling below 50 mb is not shown since their global mean water vapor trend approaches zero near 60 mb). Dvorstov and Solomon (orange) show peak cooling by 0.6 K near 50 mb falling to zero near 1 mb. Rind and Lonergan [*1995*] equilibrium cooling (labeled 25-k) is seen to be increasing with height from about 0.4 K at 50 mb to about 0.8 K at 1 mb, while the Shindell [*2001*] model results (labeled 33-k) show uniform cooling by about 0.3 K between 0.5 and 50 mb. The surprising result of these studies is that equilibrium cooling can be so different both in magnitude and vertical distribution for the same perturbation. As a reference for comparison, the solid black line in Fig. 1 depicts equilibrium cooling computed with a numerical k-distribution using more than 500 k-intervals.

Forster and Shine used an intermediate version of the University of Reading GCM with a wideband infrared radiation scheme developed for use in the Reading IGCM to render radiative forcings to within 5% of narrow-band model results [*Christidis, 1999*]. The Smith *et al.* [*2001*] equilibrium cooling was obtained with a 2D model using the Goody random model treatment for water vapor radiative cooling calculations [*Haigh,* 1984]. The radiation model in the Rind and Lonergan [*1995*] study is adapted from the Model II version of the GISS GCM [*Hansen et al., 1983*] which was designed as a tropospheric model with a dynamics top set at 10 mb and a radiative cap consisting of three layers with layer boundaries at 5 and 2 mb. It uses the GISS Model II 25 k-interval k-distribution parameterization which was developed to treat thermal radiation with the minimum number of intervals necessary to reproduce radiative fluxes at the top (TOA) and bottom (BOA) of the atmosphere to within about 1% of reference line-by-line calculations [*Lacis and Oinas, 1991*]. However, in adapting Model II for the middle atmosphere studies [*Rind et al., 1988*], treatment for stratospheric water vapor was not adequately parameterized to handle absorber change dependence. The Shindell [*2001*] study also uses the standard GISS radiation model but with a 33-interval correlated k-distribution which closely reproduces the line-by-line radiative cooling in the stratosphere and agrees well with the reference 500-k interval equilibrium cooling profile up to about the 0.1 mb pressure level.

The basic reason behind these large model differences in stratospheric cooling (while corresponding TOA and BOA flux differences are relatively minor) is that at thermal wavelengths stratospheric water vapor appears paradoxically to be optically thin in the sense that it absorbs only small amounts of radiative flux, while it is actually optically thick within the narrow spectral intervals where strong absorption lines are located. These lines produce radiative effects that extend to the top of the atmosphere. This behavior is evident in the high spectral resolution line-by-line profiles of spectrally resolved cooling rate for stratospheric water vapor [*Clough et al., 1992*] which show strong cooling in the water vapor rotational band (0 – 500 cm^{-1}) extending to (and above) the 0.1 mb level. One consequence of this is that the broad band radiative transfer formulation that is used by Forster and Shine [*1999*] is missing the water vapor cooling that occurs at low pressures in the stratosphere. We use GCM simulations and 1D radiative/convective (RCM) model calculations under clear-sky conditions to examine the problem.

Results

Fig. 2 shows equilibrium temperature profiles obtained by running the GCM and the reference radiation models in a 1D RCM mode under clear-sky conditions with the surface albedo set to 0.3 to simulate global mean energy balance conditions. For simplicity of comparison, CH_4 and N_2O have een sey to zero. The 25-k radiation (Fig. 2a) shows its maximum equilibrium cooling near the 1 mb pressure level, which coincides with the level of the stratospheric temperature maximum. This is indicative of optically thin behavior that could be caused by averaging the absorption by strong lines over too broad a spectral interval. In contrast, the 33-k radiation (Fig. 2b) shows minimum cooling in the vicinity of 1 mb. Perhaps contrary to expectation, this is a manifestation of optically thick behavior that arises when water vapor optical depth level within different k-distribution intervals reaches unity at different altitudes. Points above the 1 mb pressure level cool effectively to space, while points below this level cool toward the tropopause. Since the water vapor opacity increases rapidly below the tropopause, radiation from the

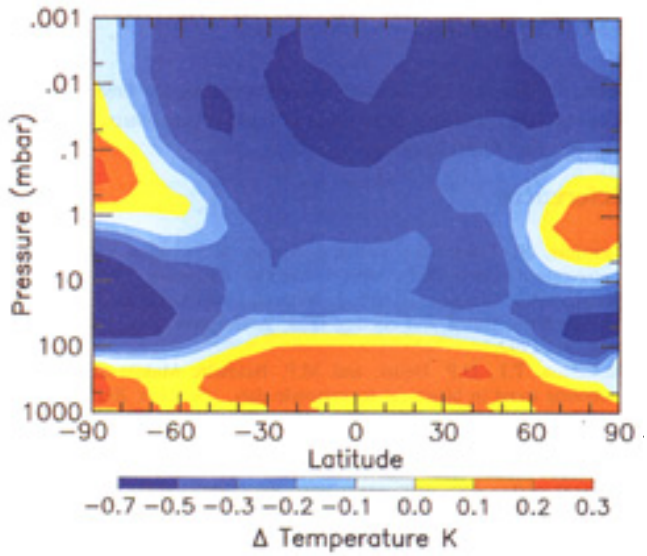

Figure 3. Pressure-latitude distribution of zonally averaged change in equilibrium temperature due to stratospheric water vapor increase above 150 mb by 0.7 ppmv over 6.0 ppmv background. Results were computed with 33 k-interval radiation using the 23-layer middle atmosphere model. ΔT differences are taken between 100-year experiment and control runs.

warmer troposphere does not interact directly with the strong water vapor lines in the stratosphere.

In Fig. 2c, equilibrium cooling profiles are computed using a high resolution numerical k-distribution model with more than 500 k-intervals. Cooling rate profiles for this model are nearly identical to line-by-line cooling rates throughout the atmosphere and thus serve as a benchmark for comparison. We note that the 33-k model shows qualitative agreement with detailed calculations while the 25-k model differs in both magnitude of cooling as well as profile shape. Studies, such as those in Fig. 2, are useful for systematically analyzing the equilibrium sensitivity of different radiation models, but they have some important limitations. For example, in 1D RCMs, the radiative tropopause occurs abruptly at about 190 mb where the critical lapse rate criterion no longer applies. This has the effect of detaching layers above 190 mb from the lapse rate constraint so they can individually attain radiative equilibrium. Thus, bottom layers of the stratosphere exhibit relative warming – actually a decrease in the temperature gradient across the tropopause boundary as opacity of the stratosphere above is increased. Sharp transitions at the tropopause do not occur in GCM simulations where the effects of atmospheric dynamics act to smooth the temperature profile [*Hansen et al., 1997b*].

Using 1D RCM results for equilibrium surface temperature change ΔT_o from Fig. 2c, and the flux conversion factor of 3.54 (as obtained from 1D RCM), we obtain the adjusted radiative forcing for uniform increases in stratospheric water vapor above 150 mb for the 500-k reference model. Expressed in Wm^{-2}, the adjusted radiative forcing is given by $\Delta F = f(x) - f(x_o)$ where

$$f(x) = 0.76 / \sqrt{1 + 0.01\,x} \; + \; 0.293\,x / (1 + 0.046\,x)\,.$$

In the above, x is in ppmv, and the formula has accuracy within 5% over the range $2 < x < 10$ ppmv. For a water vapor increase from 6 to 6.7 ppmv this yields 0.120 Wm^{-2}. For comparison the 33-k and 25-k models give 0.140 and 0.213 Wm^{-2}, and ΔT_o of 0.05 and 0.06 K, respectively. Forster and Shine [*1999*] and Smith *et al.* [*2001*] also obtain radiative forcings of 0.2 Wm^{-2} for their stratospheric water vapor increases. Thus, the radiative forcings of the different radiation models are not necessarily in direct proportion to their stratospheric equilibrium cooling.

We also test the equilibrium sensitivity of the 33-k radiation model to prescribed changes in stratospheric water vapor in a GCM context. For this we use the coarse grid 23-layer version of the GISS middle atmosphere model [Rind *et al., 1995*] with Q-flux mixed layer ocean. As in Forster and Shine, we define a control run with uniform 6.0 ppmv stratospheric water vapor above 150 mb and experiment run with 6.7 ppmv water vapor.

Experiments were run for 150 years to basic equilibrium, then continued for an additional 100 years to isolate the equilibrium response. Zonal mean temperatures were averaged over model years 151-250; the temperature difference between experiment and control runs is shown in Fig. 3. There is overall cooling of the stratosphere by about 0.3 K in basic agreement with the 1D RCM equilibrium results. There are also patterns of localized heating and cooling that are due to dynamics interactions. There is an extended region of stratospheric warming by about 0.2 K near the south pole between 0.01 and 1 mb, and a similar region toward the north pole near 1 mb. Also there are regions of enhanced cooling at low to mid latitudes form 0.01 to 0.1 mb and in polar vortex regions between 10 and 100 mb. The troposphere is generally warming by 0.1 to 0.2 K.

The global mean surface air temperature increased by 0.136 K, implying tropospheric feedback amplification of about 2.5 in response to the applied radiative perturbation of 0.14 W/m^2 that are generated by the 33-k radiation model. Direct evidence for the tropospheric feedback amplification is the decrease in global cloud cover by about 0.05% (blue dashed line, Fig. 4), and the increase in tropospheric specific humidity by about 10^{-4} (red line, Fig. 4) both of which produce tropospheric and surface warming [*Hansen et al., 1997b*].

Fig. 4 shows the globally averaged profile of the equilibrium temperature change in Fig. 3. Shown in yellow is the standard deviation of the annual-mean temperature variability of the control run for model years 151-250. For comparison, 1D RCM results for 33-k and 500-k radiation models are shown by the dotted and solid lines, respectively. As expected, there is close agreement between the 33-k GCM and 1D RCM results. The differences are due to atmospheric dynamics and seasonal and latitudinal temperature changes that are absent in the 1D RCM.

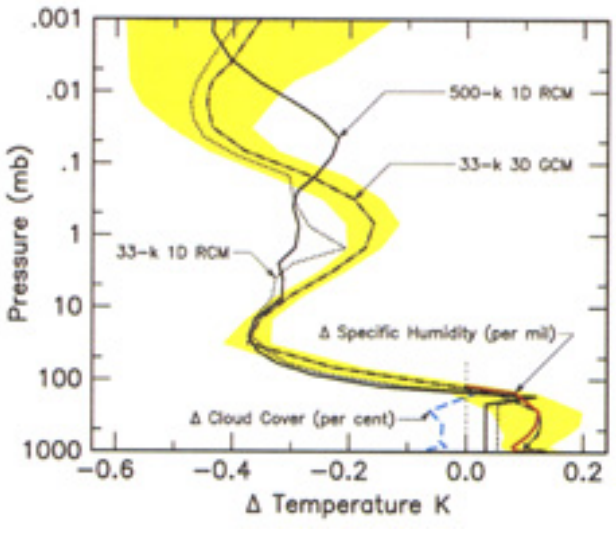

Figure 4. Global mean equilibrium temperature change (broken line) from 100-year GCM experiment in Fig. 3. Yellow margins depict the standard deviation of the annual-mean temperature change. 1D RCM results for 33-k and 500-k radiation models are shown by the dotted and solid lines. Blue dashed line depicts per cent global cloud cover change. The red line depicts the increase in global tropospheric specific humidity.

Discussion

Since the radiative forcing due to the 0.7 ppmv increase in stratospheric water vapor is small compared to the interannual model variability, long model runs are needed to isolate the signal. The increase in stratospheric water vapor by 0.7 ppmv for the 1979-1997 time period improves the closure between climate model simulations of known radiative forcings to the point where the observed stratospheric temperature trends can be explained in terms of observed changes in ozone, greenhouse gas increases, stratospheric aerosol and solar flux variations. Nevertheless, uncertainty remains because the information on stratospheric water vapor trends is not complete for the full 1979-1997 time period. The average trend of 40 ppbv/yr that was estimated by Forster and Shine [*1999*] is close to the long-term 50-year trend of 45 ppbv/yr estimated by Rosenlof *et al.* [*2001*] based on their analysis of ten different water vapor data sets. However, the trend in stratospheric water vapor increase is by no means smooth or steady. Balloonsonde measurements [*Oltmans et al., 2000*] show large decadal fluctuations in the overall trend, albeit at one geographic location and below 28 km altitude. For a more limited time period from 1992 to 1997, HALOE and WVMS measurements show the rate of water vapor increase to be as high as 129 and 148 ppbv/year at 40-60 km. Thus there remains considerable uncertainty both in the rate and vertical distribution of stratospheric water vapor change during the 1979-1997 time period. A more complete assessment of the water vapor contribution to stratospheric cooling would also take into account the changes in the vertical distribution of water vapor and include them in the GCM simulations.

Because of methane oxidation, the overall structure and variability of stratospheric water vapor and methane are closely coupled [*Randel et al., 1999*]. However, most of the observed water vapor increase appears to be due to other independent mechanisms [*Nedoluha et al., 1998; Evans et al., 1998; Zhou et al.,2001*] which might be driven by global climate change. Besides being an important contributor to the observed stratospheric cooling in the past several decades, stratospheric water vapor also has impact on the ozone distribution in the upper stratosphere [*Shindell, 2001*]. As a result, it is important to accurately define the time trend in the vertical distribution of stratospheric water vapor over past decades through further modeling and measurement analysis.

The large differences that are seen in GCM response to prescribed changes in stratospheric water vapor are clearly due to inadequacies of the radiative model parameterization of stratospheric water vapor absorption. The basic problem is that absorption by water vapor in the stratosphere is by a relatively small number of strong lines that occupy very narrow spectral intervals. Practical considerations of GCM radiation parameterizations require averaging of the water vapor absorption over relatively broad spectral intervals, typically leading to overestimated absorption. This problem can be addressed by using a correlated k-distribution approach to match line-by-line cooling rates with a sufficient number of sufficiently narrow k-intervals. While model absorption coefficients can always be tuned by appropriate absorber scaling to reproduce radiative cooling rates for a fixed atmosphere model, it will require additional absorber scaling to make the model respond properly to changes in absorber amount. Thus, for broad band parameterizations of thermal emission and transmission, this becomes increasingly more difficult for pressures characteristic of the stratosphere. The simple expedient is to increase the effective number of spectral intervals for the absorbing gas in question.

Acknowledgments. This research was supported by the Environmental Sciences Division of U.S. Department of Energy Atmospheric Radiation Measurement (ARM) Program.

References

Christidis, N., Halocarbon radiative forcing in radiation and general circulation models, Ph.D. thesis, University of Reading, 1999.

Clough, S.A., M.I. Iacono, and J.-L. Moncet, Line-by-line calculations of atmospheric fluxes and cooling rates. *J. Geophys. Res.*, **97**, 15,761-15,785, 1992.

Dunkerton, T.J., D.P. Delisi, and M.P. Baldwin, Middle atmosphere cooling trend in historical rocketsonde data. *Geophys. Res. Lett.*, **23**, 3371-3374, 1998.

Dvortsov, V.L. and S. Solomon, Response of the stratospheric temperature and ozone to past and future increases in stratospheric humidity, *J. Geophys. Res.*, **106**, 7505-7514, 2001.

Evans, S.J., R. Toumi, J. E. Harries, M.P. Chipperfeld, and J.M. Russell, Trends in stratospheric humidity and the sensitivity of ozone to these trends. *J. Geophys. Res.*, **103**, 8715-8725, 1998.

Forster, P.M. de F. and K.P. Shine, Stratospheric water vapor changes as a possible contributor to observed stratospheric cooling. *Geophys. Res. Lett.*, **26**, 3309-3312, 1999.

Golitsyn, G.S., *et al.*, Long-term temperature trends in the middle and upper atmosphere. *Geophys. Res. Lett.*, **23**, 1741-1744, 1996.

Haigh, J.D., Radiative heating in the lower stratosphere and the distribution of ozone in a two-dimensional model, *Q. J. R. Meteorol. Soc.*, **110**, 167-185, 1984.

Hansen, J.E., *et al.*, Efficient three-dimensional global models for climate studies: Models I and II. *Mon. Wea. Rev.* **111**, 609-662, 1983.

Hansen, J.E., *et al.*, Forcings and chaos in interannual to decadal climate change, *J. Geophys. Res.*, **102**, 25679-25720, 1997a.

Hansen, J., M. Sato, and R. Ruedy, Radiative forcing and climate response, *J. Geophys. Res.*, **102**, 6831-6864, 1997b.

Hansen, J., M. Sato, R. Ruedy, A. Lacis, and J. Glascoe, Global climate data and models: A reconciliation. *Science*, **281**, 930-932, 1998.

Keckhut, P., F.J. Schmidlin, A. Hauchecorne, and M.L. Chanin, Stratospheric and mesospheric cooling trend from U. S. rocketsondes at low latitude. *J. Atmos. Solar-Terr. Phys.*, **61**, 447-459, 1999.

Lacis, A.A. and V. Oinas, A description of the correlated k-distribution method for modeling nongray gaseous absorption, thermal emission, and multiple scattering in vertically inhomogeneous atmospheres. *J. Geophys. Res.*, **96**, 9027-9063, 1991.

Nedoluha, G.E., *et al.*, Increases in middle atmospheric water vapor as observed by the Halogen Occultation Experiment and groundbased Water Vapor Millimeter-wave Spectrometer from 1991–1997. *J. Geophys. Res.*, **103**, 3531-3543, 1998.

Oltmans, S.J., H. Vomel, D.J. Hofmann, K.H. Rosenlof, and D. Kley, The increase in stratospheric water vapor from balloon-borne, frostpoint hygrometer measurements at Washington, D.C., and Boulder, Colorado, *Geophys. Res. Lett.*, **27**, 3453-3456, 2000.

Randel, W.J., F. Wu, J.M. Russell III, and J. Waters, Space-time patterns of stratospheric constituents derived from UARS measurements. *J. Geophys. Res.*, **104**, 3711-3727, 1999.

Rind, D., and P. Lonergan, Modeled impacts of stratospheric ozone and water vapor perturbations with implications for high-speed civil transport aircraft *J. Geophys. Res.*, **100**, 7381-7396, 1995.

Rind, D., R. Suozzo, N.K. Balachandran, A. Lacis and G. L. Russell, The GISS Global Climate/Middle Atmosphere Model Part I: Model structure and climatology. *J. Atmos. Sci.*, **45**, 329-370, 1988.

Rosenlof, K.H., *et al.*, Stratospheric water vapor increase over the past half-century, *Geophys. Res. Lett.*, *28*, 1195-1198, 2001.

Shindell, D.T., Climate and ozone response to increased stratospheric water vapor. *Geophys. Res. Lett.* **28**, 1551-1554, 2001.

Smith, C.A., J.D. Haigh, and R. Toumi, Radiative forcing due to trends in stratospheric water vapor, *Geophys. Res. Lett.*, **28**, 179-182, 2001.

Spencer, R.W. and J.R. Christy, Precision lower stratospheric monitoring with the MSU: Technique, validation, and results1979-1991. *J. Clim.* **6**, 1194-1205, 1993.

Zhou, X.-L., M.A Geller, and M. Zhang, The cooling trend of the tropical cold point tropopause temperature and its implications, *J. Geophys. Res.*, **106**, 1511-1522, 2001.

email: voinas, alacis, drind, dshindell, and jhansen @giss.nasa.gov

(received March 7, 2001; revised May 10, 2001;
accepted May 12, 2001)